

Phase Transitions in Heat Accumulating Inorganic and Organic Materials

Study by NMR-Relaxometry and Thermoelectrometry

Kashaev R.S.-H.

Kazan State Power Engineering University,
Dep. Instrumentation and automatic electric drive
Republik Tatarstan, RF, 420107, Kazan, Esperanto
str., 62-29, kashaev2007@yandex.ru

Abstract - Using nuclear magnetic resonance relaxometry and thermoelectrometry methods were studied phase transitions (PT) and electric power generation properties of hydrate salt $\text{CaCl}_2 \cdot 6\text{H}_2\text{O}$ and isoparaffin $i\text{-C}_{22}\text{H}_{46}$. They are phase-changing materials (PCM) and can be used as heat accumulating/emitting thermal electric energy storage. Temperature and time dependences on protons of PT were determined using Portable Relaxometer NMR NP-2 at resonance frequency $\nu_0 = 14,5 \text{ МГц}$. Was discussed mechanism of PT in the form of structure-dynamic phase transitions and presented the installation of day and night thermoelectric generator on Seebeck effect and phase transitions.

Keywords - nuclear magnetic resonance relaxometry, thermoelectrometry, phase transitions, thermoelectric generator, Seebeck effect.

1. INTRODUCTION

Direct electric energy production using thermoelectric Seebeck effect in renewal electric energy sources is of great technology relevance. Use of phase transitions (PT) in phase-changing materials (PCM) has high perspectives. At the same time the discovery of PT mechanism is one of the great physic problems [1]. Its solution gives an opportunity for use of ambient temperature changes during day and night, especially in deserts, mountains and regions with continental climate. At present time such materials, named thermal energy storage systems, are widely used in air conditioning systems [2]. Phase transitions in hydrated salts and paraffins due to their low temperatures of PT [3] can also be used for power generation - transformation of heat of fusion/crystallization in electric current power as a most convenient form of energy. For this purpose can be used the thermoelectric Seebeck effect of thermoelectricity production using temperature change during the PT at heating and cooling. [4]. But PT are not studied completely and is a complicated phenomena. Noble laureate V.L.Ginsburg put it on

the seventh place among problems, needed to be solved [1]. So new devices for fine structure of PT determination is essential for qualified choose of PCM used in thermoelectric autonomous generators on Seebeck effect and phase transitions.

2. SAMPLES, APPARATUS AND METHODS

For study were used inorganic PCM - hydrated salts: $\text{CaCl}_2 \cdot 6\text{H}_2\text{O}$, $\text{Na}_2\text{SO}_4 \cdot 10\text{H}_2\text{O}$, $\text{Na}_2\text{S}_2 \cdot 5\text{H}_2\text{O}$, $\text{CH}_3\text{COONa} \cdot 3\text{H}_2\text{O}$ and such organic PCM as isoparaffin $i\text{-C}_{22}\text{H}_{46}$. Their phys-chemical properties— temperatures of melting T_{melt} °C, heat of melting, Q_m (kJ/mol) and density ρ (kg/m^3), taken from [2,3], are presented in Table 1.

Table 1- Physico-chemical properties of samples

PCM	T_{melt} (°C)	Q_m (kJ/mol)	ρ (kg/m^3)
$\text{CaCl}_2 \cdot 6\text{H}_2\text{O}$	29,7 [3];	70[3]; 190,8;	1562 (38.7 °C);
FSP 42-0006- (pharm)	29,2; 29,7; 30 [2]	171; 74,4;192 [2]	1802 (solid); 1710 (solid) [2]
$\text{Na}_2\text{S}_2 \cdot 5\text{H}_2\text{O}$	48 [3];	210 [3]; 201;	1600[3];
GOST 27068- 86	48; 48-49 [2]	209.3 ; 187 [2]	1600 (solid); 1666; 1662 [2]
$\text{CH}_3\text{COONa} \cdot 3\text{H}_2\text{O}$	58,2 [2]	260 [2]	1450 [2]
$i\text{-C}_{22}\text{H}_{46}$	44°C	52,9	774,9
H_2O , Distil- late	0 [3]	333 [2]	998 (20°C); 917 (ice) [2]

As it is seen from the table, essential dispersion of the parameters obtained by different authors. In our opinion the reason of this data dispersion is the complex form of PT in this PTM. This work – is the study by two experimental methods (NMR and thermoelectric spectrometry) the peculiarities of phase transitions in PTM.

NMR-relaxation parameters measurements

Measurements of NMR-relaxation parameters (SDP): spin-lattice T_{1i} , spin-spin T_{2i} relaxation times and corresponding proton phases populations $P_{1,2i}$ at resonance frequency $\nu_0 = 14,5 \text{ MHz}$ were realized on the Portable Relaxometer NMR NP-2 (designed and produced by Construction Bureau of Resonance Complexes Ltd, Kazan, Republic Tatarstan, RF) and

presented at fig.1 [5].

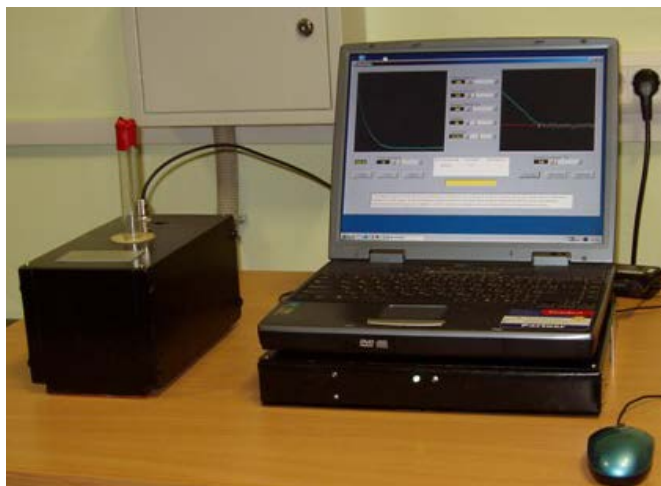


Fig.1. Portable Relaxometer NMR NP-2

Magnetic field is produced by *NdFeB* permanent magnet with field inhomogeneity $\delta H < 5 \cdot 10^{-4} B_0$ with adjustable NMR probe-head $\varnothing 30$ mm. Temperature of samples were changed and maintained with accuracy $\pm 0,2^\circ$ by thermo stabilization device, described in Patent of RF [6].

Spin-lattice T_{1i} relaxation times were determined using spin-echo recovery sequence $90^\circ\text{-}\tau\text{-}90^\circ\text{-}\tau_0\text{-}180^\circ$ of Hahn [7]. Measurement parameters were the following: pulses repetition delay time $T = 9$ s, number of pulse steps $N = 100$ with a step $\tau = 3$ ms, $\tau_0 = 200$ μ s, number of accumulations $n = 3$. For spin-spin T_{2i} relaxation times measurements $90^\circ\text{-}\tau\text{-}(180^\circ\text{-}2\tau\text{-})_N$ sequence of Carr-Purcell-Meiboom-Gill [8] was used, eliminating influence of self-diffusion and protons exchange. T_{2i} were measured with $T = 9$ s, number of 180° pulses $N = 900$, interval τ between 180° pulses – 200 μ s, $n = 10$. Main instrumental error was $\gamma_0 = \pm 1,44$ %. Experimental error of relaxation times measurements was $\pm 3\text{-}4$ %, and NMR-signal amplitudes recurrence was ± 2 %, depending from accumulations number n . So error can be reduced in $(n)^{1/2}$ times using n accumulations. Sample probe head has diameter $\varnothing 30$ mm, so the sample volume V with probe coil height $h = 35$ mm was $V = 25$ cm^3 , large enough for sample representation. Coefficient of sensibility $K = v^2 V$ [MHz^2cm^3] is $K = 4150$ MHz^2cm^3 , that is close to $K = 1600\text{-}6400$ MHz^2cm^3 of “Minispec pc120” (Bruker).

Spin-echo amplitudes A_e envelopes dependences in Hahn and CPMG-methods after amplitude detection can be described by equations:

$$A_e = 1 - \sum A_{1i} \exp(-t/T_{1i}) \quad (1)$$

$$A_e = \sum A_{2i} \exp(-t/T_{2i}) \quad (2)$$

where A_{1i} and A_{2i} (in arbitrary units) correspond to initial amplitudes of proton *A* and *B* phases of different types of water protons motions which determine relaxation times T_{1i} and T_{2i} . From measured spin-echo am-

plitudes data logarithms were taken, and the curves were decomposed on three linear components, corresponding to $T_{1,2A}$ and $T_{1,2B}$.

Term “proton phase” does not correspond to aggregate state, but to protons concentrations $P_{1,2i}$ with corresponding relaxation times $T_{1,2i}$.

For sufficient number of experimental points (> 100), reverse Laplace transformation (L^{-1}) can be used and the time dependence of signal ($A_e = \sum A_{2i} \exp(-t/T_{2i})$) can be transformed in function of T_{2i} appearance probability [9] using *CONTIN*, *DASHA*, *UPEN* and other programs. So the relaxation times distribution can be determined. However, there exists the demand of noise low level $S/N < 100$ to avoid displacements of $T_{1,2i}$ values and distortions of weight coefficients. Such level of S/N is usual case in experiment. At $S/N = 10$ L^{-1} transformation will give error 20% [10]. At the same time relaxation function can be approximated by the sum of exponents if $T_{1,2i}$ difference is large enough [11]. It is our case, and for relaxation times determination we used graph-analytical spin-echo envelopes dependences decomposition, described in [12].

Molecular motion activation energies E_A derived from the linear parts of T_1 and T_2 from reverse temperatures ($10^3/T$) dependences were determined. At high temperature approximation $2\pi\nu_0\tau_c \ll 1$ correlation times τ_c (time of living of protons in definite position) can be described by Arrhenius equation $\tau_c = \tau_0 \exp(E_A/RT)$, where τ_0 - period of atoms oscillations, $R = 8,314$ J/mol – universal gas constant. In this approximation, intramolecular contribution in relaxation the activation energy E_A can be determined using values of relaxation times $T_{1,2}^{(2)}$ and $T_{1,2}^{(1)}$, measured at temperatures $T^{(1)}$ and $T^{(2)}$ [13]:

$$E_A \text{ (J/mol)} = 19,13 \lg(T_{1,2}^{(2)}/T_{1,2}^{(1)}) [T^{(1)}T^{(2)}/(T^{(2)}-T^{(1)})] \quad (3)$$

Error of E_A determination is estimated equal to ± 5 %.

Thermoelectric measurements

Techniques used to study phase transitions are usually conventional calorimetric, differential scanning calorimetric (DSC) and differential thermal analysis (DTA). As it was mentioned by Gibbs [ref.71 in 2], there is considerable uncertainty about the property values provided by manufacturers. Yinping [ref.72 in 2] reviewed conventional calorimetric methods and pointed out their limitations such as: a) too small quantities of sample analyzed (1-10 mg), although some properties depends on sampler volume; b) phase changes cannot be visually observed. According to [14] error of DTA-method reach $\pm 3\%$ at measurement range ends. Taking this in consideration we elaborated (described in [4, 15]) TE-device as combination of the common and differential calorimetry additionally determining Seebeck thermoelectric tension U and current I of endo/exothermic effects in great volumes from temperature and time,. It may be called thermoelectrometry (TE) method to reveal the fine

structure of phase transitions.

Thermoelectric element TEC-127-06C was used, one solder of which is connected with heat conducting plate, immersed in sample. Another solder is connected with radiator, blown by cooler or freeze by melting ice. Cooling process was controlled during up to 360 minutes in the sample of volume $V \approx 100$ ml. Temperatures in sample and water were measured by TE and precision thermo resistors in the temperature range $-50 \text{ }^\circ\text{C} \leq T \leq +180 \text{ }^\circ\text{C}$. Measurement error $\pm 0.2 \%$.

3. EXPERIMENTAL RESULTS

3.1. Experimental results of NMR-relaxation measurements

Results of measurement of spin-lattice T_{1A} , T_{1B} and spin-spin relaxation T_{2A} , T_{2B} times from inverse temperature $10^3/T$ K and time in $\text{CaCl}_2 \cdot 6\text{H}_2\text{O}$ are presented at fig.2,3.

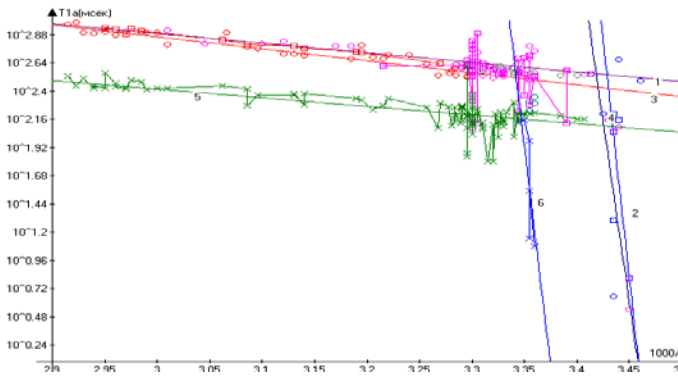


Fig.2. Temperature dependences of relaxation times from inverse temperature $10^3/T$ in $\text{CaCl}_2 \cdot 6\text{H}_2\text{O}$ Curves 1,2 – T_{1A} ; curves 3,4 – T_{2A} ; 5,6 – T_{2B}

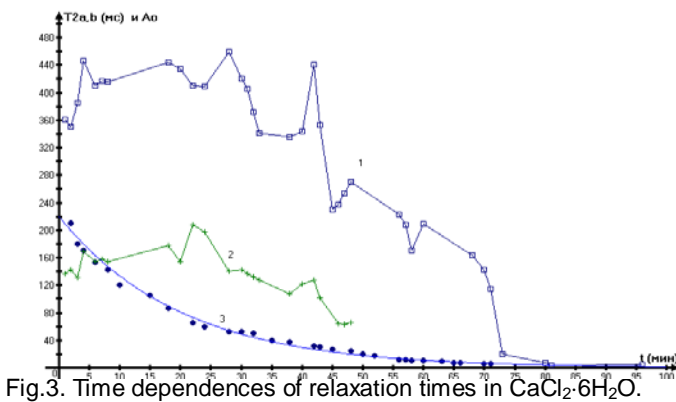


Fig.3. Time dependences of relaxation times in $\text{CaCl}_2 \cdot 6\text{H}_2\text{O}$. Curves 1,2 – T_{2A} , T_{2B} ; curve 3 – A_0

Experimental results of NMR-analysis of $i\text{-C}_{22}\text{H}_{46}$ are presented at the figs. 4 and 5 as the temperature (fig. 4) and time (fig. 5) dependences of relaxation times.

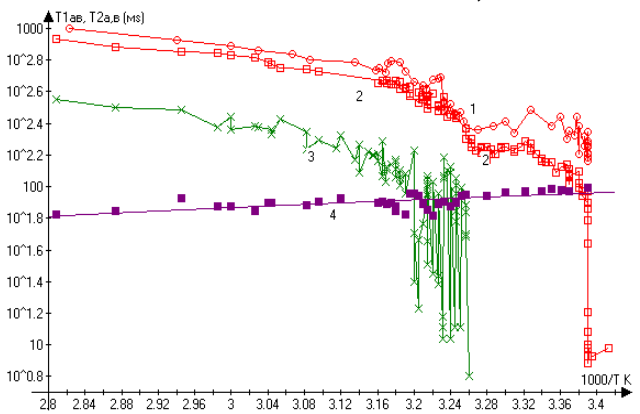


Fig.4. Temperature dependence of spin-lattice T_{1A} (curve 1), spin-spin $T_{2A,B}$ (curves 2, 3) relaxation times from $10^3/T$ K and P_{2A} proton population (line 4) at cooling of $i\text{-C}_{22}\text{H}_{46}$.

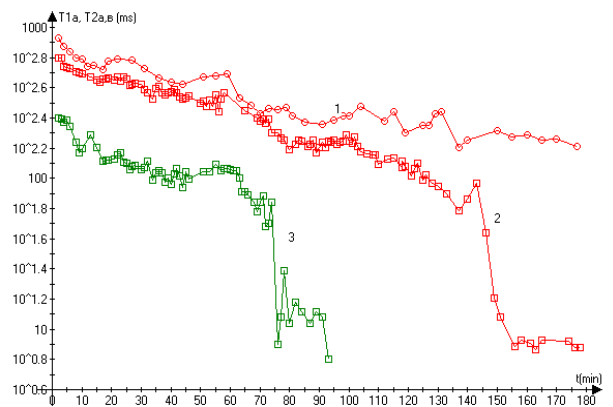


Fig.5. Time dependences of spin-lattice T_{1A} (curve 1), spin-spin $T_{2A,B}$ (curves 2, 3) relaxation times from time t of $i\text{-C}_{22}\text{H}_{46}$ cooling

3.2. Experimental results of TE-measurements

Results of TE-measurements in inorganic PCM are presented at fig.6 as a time dependences of thermoelectricity tension $U(t)$ of $\text{CaCl}_2 \cdot 6\text{H}_2\text{O}$ and water .

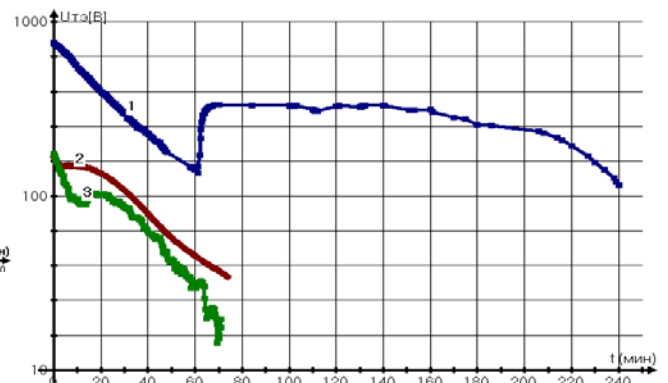


Fig.6. Time dependences of thermoelectricity - electric tension of $\text{CaCl}_2 \cdot 6\text{H}_2\text{O}$ (curve 1), $\text{Na}_2\text{S}_2\text{O}_3 \cdot 5\text{H}_2\text{O}$ (curve 2) and $\text{CH}_3\text{COONa} \cdot 3\text{H}_2\text{O}$ (curve 3) at cooling process

As it is seen from fig. 6 thermoelectric curves have complex form and at exothermic phase transitions demonstrate different temperature increments $\Delta T_e(T)$ followed by plato for different samples. Maximal exothermic temperature T_e peak appear for $\text{CaCl}_2 \cdot 6\text{H}_2\text{O}$ (curve 1), at 60-th minute. Compare $\text{CaCl}_2 \cdot 6\text{H}_2\text{O}$ exothermic temperature increment with the such in $\text{Na}_2\text{S}_2 \cdot 5\text{H}_2\text{O}$ and $\text{CH}_3\text{COONa} \cdot 3\text{H}_2\text{O}$ (see Table 2) it can be seen, that $\Delta T_e(T)$ increases with number of hydrated water molecules sited in tetrahedral voids of crystal, giving maximal thermoelectric tension $\Delta U = 750 \text{ mV}$ on TEC-127-06C constructed from modern material and with greater square of surface.

So, from the position of most effective phase changing inorganic material is $\text{CaCl}_2 \cdot 6\text{H}_2\text{O}$

Results of thermoelectric measurements as dependence of temperature T_D ($^\circ\text{C}$) of $i\text{-C}_{22}\text{H}_{46}$, water (it has no phase transitions in this temperature range) and voltage $U(\text{mV})$ of thermo element (thermoelectric force) from time t of cooling are presented at fig. 7

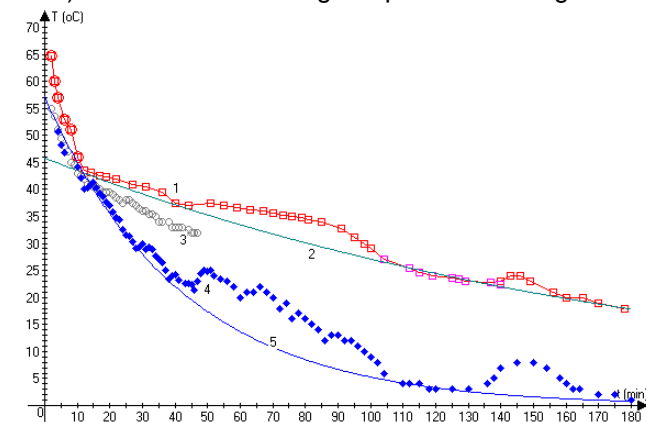


Fig.7. Time dependence of temperature T_D ($^\circ\text{C}$) of $i\text{-C}_{22}\text{H}_{46}$ (curve 1), water (curve 3), voltage $U(\text{mV})$ (curve 4) at cooling. Curves 2 and 5 - base lines for T_D ($^\circ\text{C}$) and $U(\text{mV})$.

As it is seen from fig.7, voltage $U(\text{mV})$ curve demonstrate several exothermic peaks at different times of cooling. So $i\text{-C}_{22}\text{H}_{46}$ paraffin has heat accumulating properties stretched in time and relatively lower than in $\text{CaCl}_2 \cdot 6\text{H}_2\text{O}$ voltage increments.

4. DISCUSSION

Relaxation rate $(T_{1,2})^{-1}$ of protons has two contributions: intramolecular

$$(T_{1,2})^{-1}_{\text{intra}} = 3\gamma^4 h^2 \tau / 8\pi^2 R_{ij}^6, \quad (4)$$

which characterize relaxation, caused by reorientations of water or $-\text{CH}_3$ molecules in crystalline structure, and intermolecular contribution:

$$(T_{1,2})^{-1}_{\text{inter}} = \pi\gamma^4 h^2 N \tau_D (1 + 2a_0/5D\tau_D) / 4a_0^3, \quad (5)$$

caused by translation diffusion of water in the melt or reorientation of paraffin $-\text{CH}_2$ -chains [13], where $\gamma/2\pi = 4256/\text{sec}\cdot\text{gauss}$ – gyromagnetic ratio for protons, $h = 6,626 \cdot 10^{-34} \text{ J}\cdot\text{s}$ – Plank constant, $N_i = 6,75 \cdot 10^{28} \text{ m}^{-3}$ – number of spins in cm^3 , a_0 – average molecular diam-

eter, R_{ij} – average distance between protons, τ_R and τ_D – correlation times of rotational and translational motions ($\tau_D = a_0/12D$), D – self diffusion coefficient of water molecules. Inter-proton distances R_{ij} can be calculated using eq(5).

Studied crystal-hydrate $\text{CaCl}_2 \cdot 6\text{H}_2\text{O}$ is of the type, in which water molecules sited directly on the ions, not in the pores or channels. That's why the main relaxation is caused by reorientations of water molecules $(T_{1,2})^{-1}_{\text{intra}}$ connected by hydrogen H-bonds. More long times T_{1A} and T_{2A} of proton phase A are attributed to protons of non crystallized bulk water, times T_{1B} , T_{2B} – to the B phase with definite degree of crystal state through H-bonds. Analysis gives opportunity to make a conclusion (as it was noted by [16]), that relaxation is determined not only by the factor of overcoming of activation energy of potential barrier, but depends also from entropy factor, connected with molecular ordering. Salt crystal structure repeat water tetrahedral structure with $104^\circ 27'$ angle between $\text{O-H}\dots\text{O}$ bonds.

As it is seen from fig.7 phase transition in $\text{CaCl}_2 \cdot 6\text{H}_2\text{O}$ takes place in the oscillating form in wide temperatures range $T = 16\text{-}26^\circ\text{C}$ ($10^3/T = 3.46\text{-}3.375$) and finish at $10^3/T = 3.375$ and 3.46 for phase B and A by fall of relaxation times.

Temperature dependences of T_{1A} , T_{2A} and T_{2B} from $1000/T$ are characterized by exponents and in frame of coordinates $\lg T_{1,2i}$ ($10^3/T$) presented for T_{1A} by two lines with individual energies of activation E_A – in high and low temperature range. Two proton phases A and B with different activation energies are observed even in pure water near phase transition [13, c.114]. For high temperature E_A of water protons and E_A determined for crystal-hydrate from T_1 are very close: 3,7 and 3,79 kcal/mole respectively.

Temporary dependences of relaxation times on fig.5 in during the phase transition are also complicated. Relaxation times of the both phases A and B change in oscillating form. So, on curve 1 (squares) - T_{2A} and on curve 2 (crosses) - T_{2B} several extremes of relaxation times are observed. That mean - phase transition of crystallization take place not in a moment, but is prolonged for time. The full crystallization at cooling process does not happen at temperature $T = 30^\circ\text{C}$ (as is reported in literature), but begins at earlier temperatures and goes, passing through formation of temporal ordered structures, which gradually increase their degree of ordering and form minimum of T_{2i} as it follows from eq.(5). This process gives oscillations of T_{2i} at crystallization. Ordering from melt can be attributed to metastable state and for both A and B proton phases this temperature range is approximately in the range $30\text{-}35^\circ\text{C}$, corresponding to unstable intermediate state, which can be named structure-dynamical phase transition (SDPT). At the end of this

range, before the transition to completely ordered (crystal) state, expenditure of the heat, i.e. additional energy for transformation of water molecules in the more ordered state is needed. Decrease of T_{2A} and T_{2B} at SDPT takes place as a result of decrease of interproton distances R_{ij} at every new ordered superstructure formation, which is accompanied by exothermic process – emission of heat.

NMR signal amplitude A_0 on fig.5 (curve 3), demonstrate decrease at cooling. As it was mentioned in [17], at cooling take place lay of many structure and phase transitions, and crystallization centers grow by molecules, delayed in media due to viscosity. Crystal growth C_t process can be described by Colmogorov-Avrami equation [17]:

$$C_t = 1 - \exp(-Zt^n) \quad (6)$$

where Z – crystallization rate constant, n - coefficient, depending from crystals formation and growth mechanism (Avrami index). At $n=3-4$ three dimension crystals are formed, at $n=2$ appear fibrillar crystals. At $n=1$ formed linear dendrites.

In our case decrease of the liquid phase content characterized by NMR A_0 and can be described by exponential equation with correlation coefficient $R^2=0,99$ by equation:

$$C_t = 220.2[1 - \exp(-0.05t)] \quad (7)$$

Taking in mind, that Avrami index is $n = 1$, we can suppose, that in $\text{CaCl}_2 \cdot 6\text{H}_2\text{O}$ crystallization goes through formation of one dimensional dendrites.

It is really so - photograph on fig.8 made on digital technical 200X microscope confirm this. It is seen, that big crystals are formed by parallel oriented dendrites.



Fig.8. Photographs of crystals $\text{CaCl}_2 \cdot 6\text{H}_2\text{O}$

At temperature dependences of relaxation times T_{2i} for isoparaffin $i\text{-C}_{22}\text{H}_{46}$ at fig.4 several temperature ranges with different behavior of T_{2i} can be elucidated. They are the following:

- i) Range $10^3/T = 2,8-3,16$ ($84 - 43^\circ\text{C}$) of relatively

monotone decrease of T_{2A} and T_{2B} with the activation energies $E_{A2A} = 12.35$ kJ/mol, $E_{A2B} = 13.6$ kJ/mol (left part of the curves 1 and 2) of the paraffin melt. The end of the range at temperature 44°C of phase transition and at 43°C of allotrope transformation (coinciding with reference book data);

- ii) Below this temperature range at $10^3/T = 3,16-3,26$ ($43 - 34^\circ\text{C}$) T_{2B} of B proton phase has an uneven behavior with oscillations of T_{2B} from 10 ms to 120 ms in the structure-dynamical phase transitions range. We suppose they are caused by structure-dynamical processes of temporal ordering of structure before the final crystallization at temperature 35°C ($10^3/T = 3,25$), at which T_{2B} falls to stable value $T_{2B} = 6.3$ ms.

- iii) For relaxation times T_{2A} of A proton phase in the range $10^3/T = 3,155-3,37$ ($43 - 24^\circ\text{C}$) the decrease of T_{2A} with three clear extremes (minimums) of T_{2A} are observed. Probably they are connected with three-stage process of pre crystallization ordering of $-\text{CH}_2-\text{CH}_3-$ groups. After that at the range $10^3/T = 3,356-3,39$ ($25 - 22^\circ\text{C}$) we observe oscillation process with the amplitude of T_{2A} oscillations from 89 ms to 126 ms. Fluctuations ends at 22°C by the full crystallization of the proton phase A and sharp fall of T_{2A} to value 7.6 ms and only this temperature may be named "rigid lattice" state of paraffin.

- iiii) In the melt state of paraffine proton phase A population (corresponding to the end CH_3 -groups) has value $P_{2A} = 65\%$. At the temperature of the full cooling its value reach value $P_{2A} = 98\%$, which is interpreted as that at low temperatures main contribution in relaxation comes from the end chains. Molecular fragments of B phase $\dots\text{CH}_2-\text{CH}_2-\text{CH}_2-\dots$ have reached already solid crystallized (ordered) state [18, 19].

5. RESULTS APPLICATION - THERMOELECTRIC GENERATOR ON SEEBECK EFFECT AND PHASE TRANSITIONS

On the base of obtained results was elaborated thermoelectric generator on Seebeck effect and phase transitions [20-22], one of which is at fig.9.

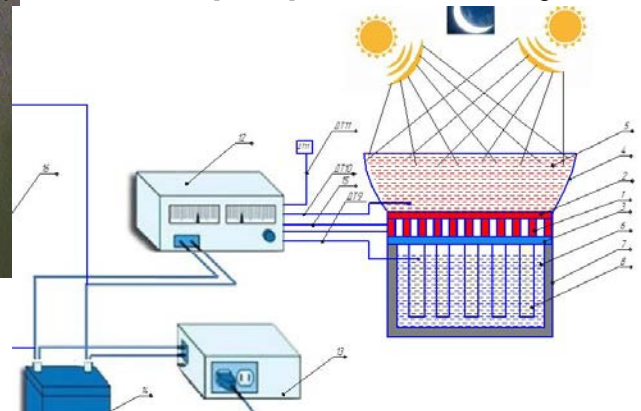


Fig.9 Thermoelectric generator on Seebeck effect and phase transitions

In the device used battery of N thermoelements

(TE TEC-127-06C) 1, by "hot" solder 2 contacting with thermal/sun collector 4 formed from parabolic capacity with PCM I 5. In thermoelectric ambient and sun heat is accumulated in the day-time in PCM I and used by thermoelements day and night time at cooling from jump of temperature at exothermic PT. Walls of thermal/sun collector concentrate sun radiation on PCM I. Heat transferring plate is immersed in the PCM II deposited at low temperature at soil or better in flowing water. For control of current direction *Atmega* controller is used. Thermo electric tension (TET) dependence on one TE from time t of operationshow, that TET reach value 0.75 V at day-time heating up to temperature $T = 65\text{ }^{\circ}\text{C}$ and then at night-time decrease with cooling of PCM I. But on 240-th minute it experiences exothermic PT giving jump of TET on 0.35 V. Choose of several PCM with different phase transition temperatures able day and night receive maximal electric tension on thermoelements multiple to N TE.

To increase of thermo effect and prolong it several PCM can be used, for instance $\text{CaCl}_2 \cdot 6\text{H}_2\text{O}$, $\text{Na}_2\text{S}_2\text{O}_3 \cdot 5\text{H}_2\text{O}$ and $\text{CH}_3\text{COONa} \cdot 3\text{H}_2\text{O}$ with different PT temperatures $T_{\text{фп}} = 30, 48$ и $58\text{ }^{\circ}\text{C}$.

6. CONCLUSIONS

1. In temperature dependences of both $\text{CaCl}_2 \cdot 6\text{H}_2\text{O}$ and paraffin $i\text{-C}_{22}\text{H}_{46}$ relaxation times demonstrate different behavior at the cooling process. Relatively monotone decrease of relaxation times changed by oscillations, followed by the final sharp fall of T_{2i} to the value in the crystal state. This is, we suppose, the indication of the ordering of first B and then A proton phases.

2. Solidification process for hydrated salt and paraffin on thermoelectrodynamical curve demonstrate sharp increase, corresponding to exothermic heat emission. At the same temperatures the extremes are observed on the thermo-element tension U_{TE} (mV) dependence. Peculiarities in T_{2i} and caloric curves behavior can be explained by structure-dynamical phase transitions (SDPT), which appear as a result of temporary (dynamical) formation and the following destruction (melting) of the supermolecular structures clusters.

3. SDPTs are accompanied by the decreasing of R_{ij} as a result of ordering and increasing of its density. Final phase transition do not end at $T = 29\text{-}30\text{ }^{\circ}\text{C}$, but goes on to the lower temperatures up to $16\text{ }^{\circ}\text{C}$, passing through formation of temporal structures, gradually increase degree of ordering.

7. REFERENCES

1. V.L.Ginzburg <http://ginzburg-ocr.narod.ru/online/ginzch2.htm>
2. B.Zalba, J.M.Marin, F.Cabeza, Mehling H. Review of thermal

energy storage with phase change: materials, heat transfer analysis and applications. Applied Thermal Engineering v.23, pp.251-283, 2003.

3. Chemist's reference book, V.1, L.-M.: 1963.
4. R.S.-H.Kashaev, A.G.N. Masiab Device for phase transitions temperature measurement. Patent of Russian Federation №136894 RF, *G01R7/00*. 2013; publ. Bulletin of Inventions RF. 20.01.14, № 2.
5. Z.Sh.Idiyatullin, R.S.-H.Kashaev, A.N.Temnikov, Patent of Russian Federation № 67719, *G01N24/05* 2006.
6. Z.Sh.Idiyatullin, R.S.-H.Kashaev, A.N.Temnikov, Patent of Russian Federation №23191138. 4.05.2006.
7. E.L. Hahn. J.Geogr.Res. vol.65, p.776, 1960.
8. S.Meiboom, D.Gill. Review of Scientific Instruments. Vol.29, p. 688,1958.
9. S.W.Provencher. Comp.Phys.Comm. vol.27, p. 229 1982.
10. A.M. Perepuchov. Algorithm of reverse Laplace transformation for complex relaxation data processing. Abstracts of International Scientific Conference. St.Petersburg University. p.98, 2010.
11. R.J.S. Brown. Information available and unavailable from multiexponential relaxation date J.Magn.Res. vol.82, pp. 539-561,1989.
12. R. S.-H.Kashaev, E.G. Gazizov. Operative control of the bitumen and oil components by the NMR-metod. Izvestiya VUZov. Problemy energetiki. Vol. 7,8, p.7, 2010.
13. A.A.Vashman, I.S. Pronin. Nuclear magnetic relaxation and its use in chemical physics. -M.: Nauka, 1979. -235 p.
14. J.E.Callaghan, S.A. Sullivan. Rev. Sci. Instr. Vol.57, #10, pp.2584-2592, 1986.
15. R. S.-H.Kashaev, A.G.N. Masiab. Phase transitions in some phase changing organic materials studied by nuclear magnetic resonance relaxometry. Chemical and Materials Engineering. V. 1(3), pp.78-84, 2013.
16. Yu.I.Moskvich, N.A.Sergeev, G.I. Dotcenko. Study of water mobility in sorrel acid by NMR method. Journal of Structure Chemistry. Vol.19,pp. 57-63, 1978.
17. A.Sharpleze. Crystallization of polymers. MIR publishing. M.: 1968.
18. R. S.-H.Kashaev, A.G.N. Masiab. Phase transitions – source of electric energy. Energetic of Tatarstan. №4. pp.347-354, 2013.
19. R. S.-H.Kashaev, A.G.N. Masiab. Day and night autonomous source of electric energy, using ambient temperature.Fundamental researches. №10. pp.1724-1729, 2013.
20. R. S.-H.Kashaev, A.G.N. Masiab. Phase transitions in some phase changing organic materials studied by nuclear magnetic resonance relaxometry. Chemical and Materials Engineering., Vol. 1(3), pp.78-84,2013.
21. R. S.-H.Kashaev, A.G.N. Masiab. Thermoelectric generator. Patent of RF № 135450, *H01J45/00, F24J2/42.*; Bulletin of inventions. № 34.
22. R. S.-H.Kashaev, A.G.N. Masiab. Thermoelectric autonomous source of energy. Patent of RF № 135450 RF, *H01J45/00*; Bulletin of inventions. № 32.